Chemical Engineering Journal 112 (2005) 227–236

Chemical Engineering Journal

www.elsevier.com/locate/cej

Kinetics and thermodynamics of the organic dye adsorption on the mesoporous hybrid xerogel

Zhijian Wu [a,b], Hyeonwoo Joo [a], Kangtaek Lee [a,*]

[a] *Department of Chemical Engineering, Yonsei University, 134 Shinchon-dong, Seodaemun-gu, Seoul 120-749, Republic of Korea*
[b] *College of Materials Science and Engineering, Huaqiao University, Quanzhou 362011, PR China*

Received 1 June 2004; received in revised form 7 July 2005; accepted 12 July 2005

Abstract

We investigate the kinetics and thermodynamics of brilliant blue FCF (BBF) adsorption on a mesoporous hybrid xerogel derived from tetraethoxysilane (TEOS) and propyltriethoxysilane (PTES) with cetyltrimethylammonium bromide (CTAB) as a templating agent. We study the effect of initial BBF concentration, temperature, pH, and ionic strength on the adsorption of BBF from aqueous solution. Kinetic studies show that the kinetic data are well described by the pseudo second-order kinetic model. Initial adsorption rate increases with the increase in initial BBF concentration and temperature. The internal diffusion appears to be the rate-limiting step for the adsorption process. The equilibrium adsorption amount increases with the increase in initial BBF concentration, temperature, solution acidity, and ionic strength. The thermodynamic analysis indicates that the adsorption is spontaneous and endothermic. Electrostatic attraction and hydrophobic interaction are suggested to be the dominant interactions between dye and the xerogel surface.

Keywords: Brilliant blue FCF; Mesoporous hybrid xerogel; Adsorption kinetics; Adsorption thermodynamics

1. Introduction

Selective adsorption has become increasingly important in recognition, sensing, and separation of molecules and ions. An adsorbent with high adsorption capacity and good selectivity is very critical in adsorptive separation in which pore size control and surface modification are the two key problems. In the preparation of improved adsorbents for specific substances, increasing the pore size enables the adsorption of larger molecules and ions, since the small pores of microporous adsorbents restrict their application to only smaller organic molecules (C_3–C_7) [1]. Furthermore, narrow pore size distribution enables the adsorbents to have a good size selectivity through a sieve effect. Surface modification is very helpful for the improvement of the adsorption capacity and selectivity of the adsorbents by taking advantage of specific interactions between the adsorbents and the adsorbates. Based on these considerations, functionalized mesoporous oxides have been regarded as effective adsorbents [2–9] because of their high surface area, the functionalized pore channels of large diameter and volume, and narrow pore size distribution. The high surface area allows the binding of a large number of surface groups, and the functionalized pore channels of large diameter and volume allow an easy adsorption of specific adsorbates.

The grafting of the functional groups to the pore walls of the mesoporous adsorbents can be achieved by the reaction between the hydrolyzable moieties and the surface silanol groups of the mesostructures. Although this method has been used for a design of new adsorbents and catalysts, it has two major shortcomings: (1) it is difficult to control the loading of the functional groups; (2) during surface modification or grafting, unwanted polycondensation by-products can be easily formed. Direct incorporation of functional groups onto mesoporous silica adsorbents is an alternate route for the preparation of such materials in which the templates could be removed by solvent extraction without damaging the silica frameworks. Unlike the grafting process, direct incorporation allows the functionalized mesoporous adsorbents to retain

* Corresponding author. Tel.: +82 2 2123 2760; fax: +82 2 312 6401.
E-mail address: ktlee@yonsei.ac.kr (K. Lee).

1385-8947/$ – see front matter © 2005 Elsevier B.V. All rights reserved.
doi:10.1016/j.cej.2005.07.011

Nomenclature

A	pre-exponential factor ($g\,mol^{-1}\,s^{-1}$)
C	liquid-phase concentration at time t ($mmol\,L^{-1}$)
C_{Ae}	adsorbed amount per liter of solution at equilibrium ($mmol\,L^{-1}$)
C_e	liquid-phase concentration at equilibrium ($mmol\,L^{-1}$)
C_0	initial liquid-phase concentration ($mmol\,L^{-1}$)
E_a	activation energy of adsorption ($kJ\,mol^{-1}$)
ΔG°	Gibbs free energy change of adsorption ($kJ\,mol^{-1}$)
ΔH°	enthalpy change of adsorption ($kJ\,mol^{-1}$)
k	adsorption rate constant (h^{-1} for first-order adsorption, $g\,mol^{-1}\,s^{-1}$ for second-order adsorption)
k_{id}	internal diffusion constant ($mmol\,kg^{-1}\,h^{-1/2}$)
K_c	adsorption equilibrium constant
K_F	Freundlich equation constant
K_L	Langmuir equation constant ($L\,mmol^{-1}$)
m	xerogel mass (kg)
$1/n$	adsorption intensity for Freundlich equation
q	adsorption amount at time t ($mmol\,kg^{-1}$)
q_e	adsorption amount at equilibrium ($mmol\,kg^{-1}$)
q_m	maximum adsorption amount ($mmol\,kg^{-1}$)
r	correlation coefficient
R	gas constant ($J\,mol^{-1}\,K^{-1}$)
ΔS°	entropy change of adsorption ($kJ\,mol^{-1}\,K^{-1}$)
t	time (h)
$t_{1/2}$	half-adsorption time (h)
T	temperature (K)
u	initial adsorption rate ($mmol\,kg^{-1}\,h^{-1}$)
V	solution volume (L)

Greek letters

θ	dimensionless time, i.e. $t/t_{1/2}$
ξ	dimensionless adsorption amount, i.e. q/q_e

high surface area and pore volume, to have a uniform functional group distribution inside the pore channels, and to avoid the local clustering of the functional groups and the necking of the pore channels.

One practical problem with both procedures is, though, that the resulting materials are typically comprised of small particles. These particles are difficult to handle and must be bound to an inert material such as kaolin clay for use in packed beds. This leads to an increased bed volume and a reduction in mass transfer rates. Thus, it would be desirable to develop hybrid materials that are self-supported, while still retaining their other favorable properties. Sol–gel technology provides a viable approach to design stable, optically transparent host matrices for sensor, optical, chromatographic, and catalytic applications. In this paper, we develop a one-step synthesis of a mesoporous hybrid xerogel in which pore size and hydrophobicity are controlled by adding surfactants and an organosilane, respectively. This material is self-supported and easy to handle.

In order to predict and design the adsorption process, it is important to understand the adsorption kinetics and thermodynamics. Although the different types of functionalized mesoporous oxides have been used for the adsorption of biomolecules [2,3], heavy metal ions [4,5], and organic pollutants [6–9], little work has been done to study the adsorption kinetics and thermodynamics. Compared with the conventional adsorbents, the mesoporous hybrid adsorbents have the mesopores of narrow size distribution and modified surfaces, giving them their own adsorption characteristics. Studying the adsorption kinetics and thermodynamics of the hybrid mesoporous adsorbents is not only helpful for the understanding of the adsorption process itself, but also important for the design of new adsorbents. In this work, a mesoporous hybrid SiO_2 xerogel with propyl groups was prepared through the direct incorporation method. An organic dye, BBF, was then used as a model adsorbate to study the adsorption kinetics and thermodynamics under various experimental conditions.

2. Experimental

2.1. The xerogel adsorbent

The xerogel adsorbent was prepared through a two-step sol–gel process. Forty-four millilitres of TEOS and 46 mL of PTES (Aldrich), 300 mL of ethanol, 22.4 mL of H_2O, 3.2 mL of 0.010 M HCl and 7.2 g of CTAB (Avocado) were mixed and stirred to get a transparent sol. This sol was hydrolyzed in a covered beaker for 3 days at room temperature before 2.4 mL of 1.0 M ammonia was added. The final molar ratio was (TEOS + PTES):water:ethanol:CTAB:HCl:NH_3 = l:4:13:0.05:8×10^{-5}:6×10^{-3} where TEOS:PTES = 1:1. After gelation the gel was dried for 7 days at room temperature, followed by extraction with 200 mL of 2 M HCl in water/ethanol solution (the volume ratio between water and ethanol was 1:5) for three times at ca. 60 °C. The gel was then repeatedly soaked with water until the pH of the water after soaking was higher than 6. The soaked gel was dried at room temperature for 24 h, and finally dried at 50 °C for 2 days. The xerogel with the average diameter of ca. 1.0 mm was used for the adsorption experiments.

Textural properties of the gel were estimated using nitrogen adsorption/desorption experiments. The adsorption/desorption isotherms of nitrogen at 77 K were measured with an automated ASAP 2010 apparatus (Micromeritics, USA). Prior to the measurement the gel was degassed for 2 h at 120 °C. The specific surface area was calculated to be $588\,m^2\,g^{-1}$ from the BET equation. Average pore size and pore volume were calculated to be 2.11 nm and $0.318\,cm^3\,g^{-1}$

(mesopore volume of 0.159 $cm^3\,g^{-1}$) respectively by BJH method based on the desorption branch of the isotherm.

2.2. Properties of BBF

BBF is classified as a triphenylmethane dye with a molecular dimension of 1.07 nm × 1.47 nm × 1.88 nm [10]. Its solubility in water is 200 g L^{-1} in the temperature range of 2–60 °C. BBF has sulfonate groups that can dissociate in aqueous solution depending on the solution pH. According to the pK_a values of the sulfonate groups (i.e. 6.58 and 5.83) [11,12], the dye molecule appears as a monovalent or bivalent anion or in neutral form. In aqueous solution, BBF has a maximum absorption at 630 nm, which is very insensitive towards the solution pH and ionic strength, so the transmission is not affected over the wide range of pH (2–11) and ionic strength (0–0.1 $CaCl_2$) [13]. In our experiments, the absorption of BBF in 0.01 M HCl and 0.25 M KNO_3 solution without the addition of the xerogel at 75 °C was found to be quite stable even after 6 days.

2.3. Adsorption studies

In the adsorption experiments, 0.2 g of xerogel was mixed with 10 mL solution at the desired dye concentration, pH, ionic strength, and temperature. The adsorption experiments were carried out using a BS-06 shaking water bath (Jeio Tech, Korea) with a shaking speed of 80 rpm. Solution pH was adjusted with dilute HCl and NaOH solutions, and the solution ionic strength was adjusted with KNO_3 solution. Dye concentration change was recorded by a UV-160A Shimadzu UV–vis spectrophotometer (Shimadzu, Japan) at the maximum wavelength of BBF absorption (i.e. 630 nm). The amount of dye adsorbed onto the xerogel was calculated by a simple mass balance relationship:

$$q = \frac{V(C_0 - C)}{m} \quad (1)$$

when C_e is used instead of C in Eq. (1), q_e is obtained.

3. Results and discussion

3.1. Adsorption kinetics

3.1.1. Equilibrium time

The amount of BBF adsorbed is shown as a function of time in Fig. 1. As shown in Fig. 1, adsorption occurs more rapidly at higher temperature: it takes only <2 days to reach the adsorption equilibrium at 75 °C, while it takes ca. 6 days at 25 °C. Initial dye concentration does not have a significant effect on the equilibrium time. This is in agreement with the adsorption results of methyl violet onto perlite [14]. Thus, the time for adsorption equilibrium was set to 6 days for the adsorption thermodynamics experiments.

3.1.2. Adsorption kinetic models

Both pseudo first- and second-order adsorption models were used to describe the adsorption kinetics data [15,16]. In both models, all the steps of adsorption such as external diffusion, internal diffusion, and adsorption are lumped together and it is assumed that the difference between the average solid phase concentration and the equilibrium concentration is the driving force for adsorption, and that the overall adsorption

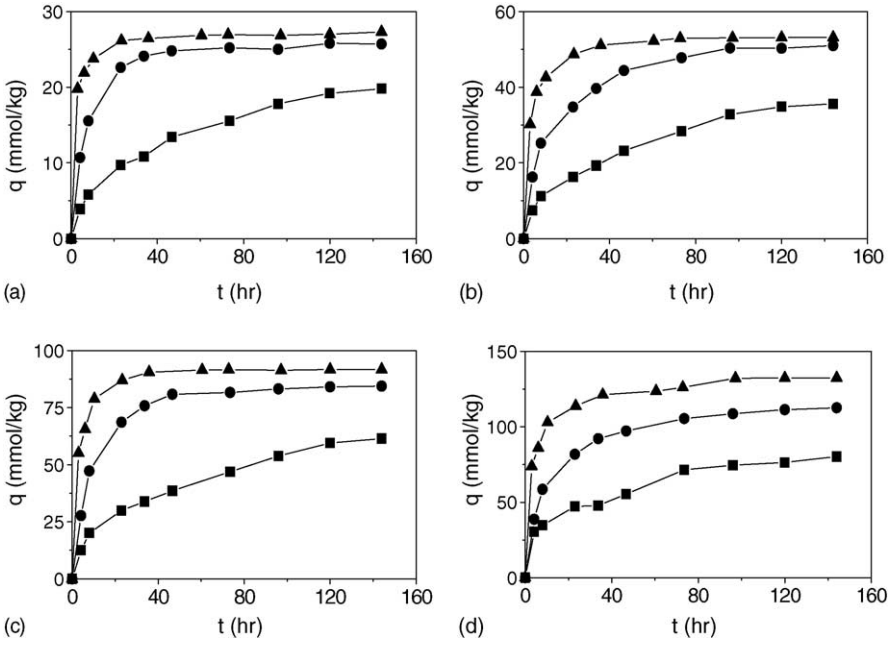

Fig. 1. Effect of the initial BBF concentration and temperature on the adsorption kinetics. Initial HCl concentration is 0.01 M; initial KNO_3 concentration is 0.25 M; initial BBF concentration is (a) 0.6 mM, (b) 1.2 mM, (c) 2.4 mM and (d) 4.8 mM. (■) 25 °C (●) 50 °C and (▲) 75 °C.

Table 1
Comparison of the experiments and the kinetic models

C_0 (mM)	Temperature (°C)	$q_{e,exp}$ (mmol kg^{-1})	First-order			Second-order		
			$q_{e,cal}$ (mmol kg^{-1})	k (h^{-1})	r	$q_{e,cal}$ (mmol kg^{-1})	k (g mol^{-1} s^{-1})	r
0.6	25	19.8	17.3 ± 1.2	0.0212 ± 0.0012	−0.993	21.3 ± 1.5	0.53 ± 0.09	0.988
	50	25.7	19.3 ± 1.6	0.0756 ± 0.0039	−0.997	31.1 ± 0.6	1.13 ± 0.16	1.000
	75	27.3	9.48 ± 1.0	0.0911 ± 0.0028	−0.999	27.7 ± 1.6	6.91 ± 2.19	1.000
1.2	25	35.6	29.9 ± 0.7	0.0191 ± 0.0006	−0.998	34.1 ± 3.4	0.41 ± 0.10	0.981
	50	51.0	37.9 ± 2.1	0.0370 ± 0.0020	−0.996	52.2 ± 2.4	0.55 ± 0.08	0.997
	75	53.2	25.1 ± 2.9	0.0760 ± 0.0088	−0.987	53.5 ± 0.7	2.18 ± 0.17	1.000
2.4	25	61.5	51.2 ± 0.1	0.0187 ± 0.0010	−0.992	62.3 ± 4.7	0.20 ± 0.04	0.986
	50	84.4	67.8 ± 4.4	0.0628 ± 0.0023	−0.998	97.5 ± 2.3	0.30 ± 0.03	0.999
	75	91.7	44.9 ± 6.9	0.0996 ± 0.0117	−0.987	96.1 ± 2.0	1.19 ± 0.14	1.000
4.8	25	80.3	59.5 ± 7.5	0.0236 ± 0.0032	−0.965	76.3 ± 9.1	0.30 ± 0.13	0.973
	50	112.6	76.5 ± 6.9	0.0365 ± 0.0032	−0.989	113.5 ± 2.0	0.31 ± 0.02	1.000
	75	132.4	59.5 ± 6.3	0.0486 ± 0.0053	−0.983	129.4 ± 2.2	0.80 ± 0.10	1.000

rate is proportional to either the driving force (as in the pseudo first-order equation) or the square of the driving force (as in the pseudo second-order equation).

$$\text{First-order model}: \ln(q_e - q) = \ln q_e - kt \quad (2)$$

$$\text{Second-order model}: \frac{t}{q} = \frac{1}{kq_e^2} + \frac{t}{q_e} \quad (3)$$

Since q reaches a plateau (q_e) at equilibrium, q values smaller than the $0.9q_e$ were used for analysis. The plots of $\ln(q_e - q)$ versus t and t/q versus t were used to test the first- and second-order models, and the fitting results are given in Table 1. According to the correlation coefficients, both models give satisfactory fits. The calculated adsorption amount at equilibrium ($q_{e,cal}$), though, shows a difference. In the first-order model, for instance, the $q_{e,cal}$ obtained from the intercepts is inconsistent with the experimental data $q_{e,exp}$, especially at 75 °C. In the second-order model, though, the $q_{e,cal}$ agrees reasonably well with the experimental data. Thus, the second-order model is more suitable to describe the adsorption kinetics data. The relationship between t/q and t for the second-order adsorption is demonstrated in Fig. 2. Similar results were observed in biosorption of dye Remazol Black B, RB2, and PY2 on biomass [17,18], anionic dye adsorption on cross-linked chitosan beads [16,19], and polyethylene glycol (PEG) adsorption on zeolite [20].

Based on the second-order model, the initial adsorption rate and half-adsorption time are estimated in Table 2

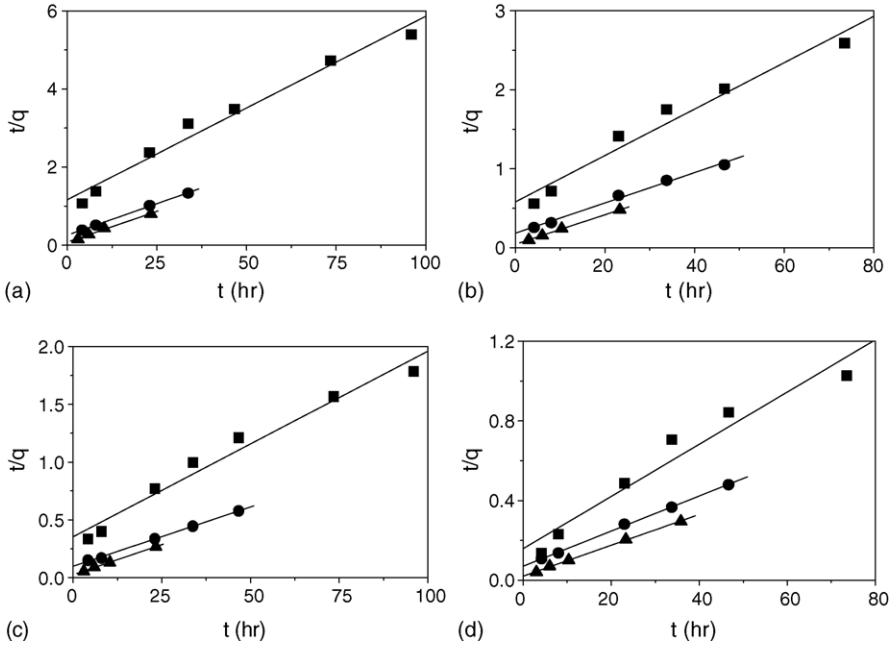

Fig. 2. The relationship between t/q and t for the second-order adsorption model. Initial HCl concentration is 0.01 M; initial KNO_3 concentration is 0.25 M; initial BBF concentration is (a) 0.6 mM, (b) 1.2 mM, (c) 2.4 mM and (d) 4.8 mM. (■) 25 °C (●) 50 °C and (▲) 75 °C.

Table 2
Kinetic parameters for the second-order adsorption model

C_0 (mM)	Temperature (°C)	u (mmol kg^{-1} h^{-1})	$t_{1/2}$ (h)	E_a (kJ mol^{-1})	r
0.6	25	0.86 ± 0.17	24.8 ± 2.5		
	50	3.85 ± 0.56	8.08 ± 1.2	43.8 ± 12.8	−0.960
	75	19.0 ± 6.2	1.45 ± 0.47		
1.2	25	1.72 ± 0.34	19.8 ± 5.2		
	50	5.42 ± 0.73	9.62 ± 1.51	28.2 ± 12.0	−0.920
	75	22.4 ± 1.7	2.39 ± 0.19		
2.4	25	2.82 ± 0.50	22.1 ± 4.9		
	50	10.2 ± 0.7	9.59 ± 0.75	30.1 ± 11.4	−0.935
	75	39.6 ± 4.4	2.43 ± 0.28		
4.8	25	6.31 ± 2.45	12.1 ± 5.3		
	50	14.2 ± 0.9	8.01 ± 0.54	16.3 ± 10.1	−0.849
	75	47.9 ± 6.0	2.70 ± 0.34		

according to the following equations:

$$u = kq_e^2 \tag{4}$$

$$t_{1/2} = \frac{1}{kq_e} \tag{5}$$

Half-adsorption time, $t_{1/2}$, is defined as the time required for the adsorption to take up half as much BBF as its equilibrium value. This time is often used as a measure of the adsorption rate.

The second-order rate constants listed in Table 1 are used to estimate the activation energy of the BBF adsorption on the xerogel using Arrhenius equation:

$$\ln k = \ln A - \frac{E_a}{RT} \tag{6}$$

The slope of plot of $\ln k$ versus $1/T$ is used to evaluate E_a, which was found to be 16.3–43.8 kJ mol^{-1} depending on the initial BBF concentration (Table 2). These values are consistent with the values in the literature where the activation energy was found to be 43.0 kJ mol^{-1} for the adsorption of Reactive Red 189 on cross-linked chitosan beads [16], or 5.6–49.1 kJ mol^{-1} for the adsorption of polychlorinated biphenyls on fly ash [21]. The second-order rate constant increases with temperature, but decreases with the initial BBF concentration. The initial adsorption rate is found to increase with the increase in the initial BBF concentration and temperature.

3.1.3. Internal diffusion analysis

The adsorption process on a porous adsorbent generally involves three stages: (i) external diffusion; (ii) internal diffusion (or intra-particle diffusion); (iii) actual adsorption [20]. Quantitative treatment of experimental data may reveal the predominant role of a particular step among the three that actually governs the adsorption rate. The adsorption step is usually very fast for the adsorption of organic compounds on porous adsorbents compared to the external or internal diffusion step [22], and it is known that the adsorption equilibrium is reached within several minutes in the absence of internal diffusion [23]. Thus, the long adsorption equilibrium time in our experiments (2–6 days) suggests that the internal diffusion may dominate the overall adsorption kinetics.

Because the above pseudo models do not provide definite information on the rate-limiting step, an internal diffusion model based on Fick's second law is used to test if the internal diffusion step is the rate-limiting step [24]:

$$q = k_{id}t^{1/2} \tag{7}$$

According to the internal diffusion model, a plot of q versus $t^{1/2}$ should give a straight line with a slope k_{id} and an intercept of zero if the adsorption is limited by the internal diffusion process [24]. The relationship between q and $t^{1/2}$ at different temperature is shown in Fig. 3. Initially in all the cases studied, a linear relationship between q versus $t^{1/2}$ with a zero intercept is found, suggesting that the internal diffusion step dominates the adsorption process before the equilibrium is reached.

To see this more clearly, we define two dimensionless variables, ξ and θ:

$$\xi = \frac{q}{q_e}; \qquad \theta = \frac{t}{t_{1/2}} \tag{8}$$

Fig. 4 shows the plot of ξ versus $\theta^{1/2}$, which clearly shows that all the data follow the same kinetics. This confirms that the adsorption process can be described by a simple internal diffusion model. For the adsorption of reactive dyes by activated carbon [25], and the adsorption of methylene blue by perlite [26], internal diffusion was found to be the rate-limiting step.

Temperature has two major effects on the adsorption process: (i) increasing temperature accelerates the diffusion of the adsorbates across the external boundary layer and in the internal pores of the adsorbents; (ii) changing temperature will change the equilibrium capacity of the adsorbent for a particular adsorbate [27]. This may result from the increase in the mobility of the adsorbates and the change of

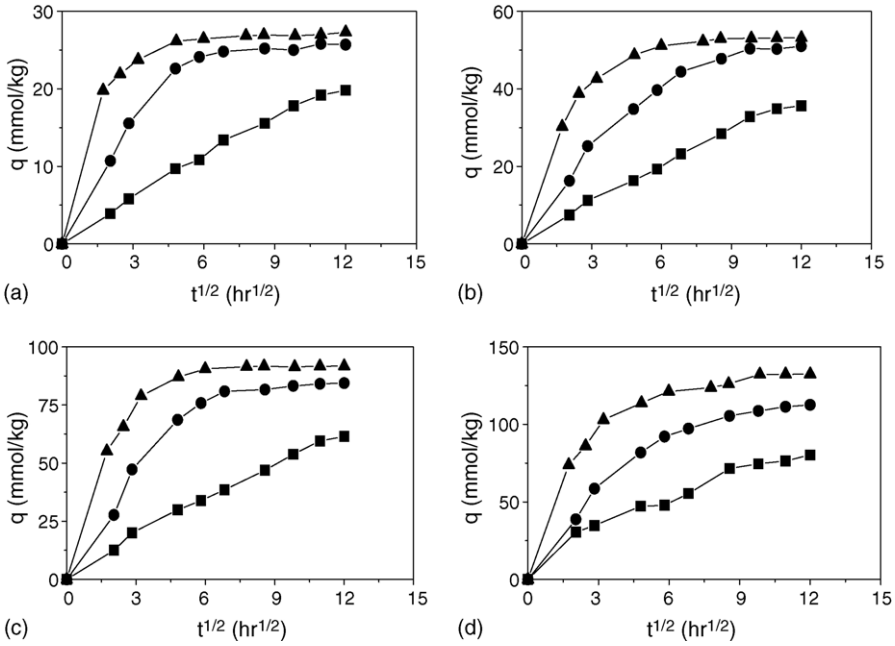

Fig. 3. Plot of q vs. $t^{1/2}$ in internal diffusion model. Initial HCl concentration is 0.01 M; initial KNO_3 concentration is 0.25 M; initial BBF concentration is (a) 0.6 mM, (b) 1.2 mM, (c) 2.4 mM and (d) 4.8 mM. (■) 25 °C (●) 50 °C and (▲) 75 °C.

the interactions between the adsorbates and the adsorbents [28]. Thus, we expect that all steps of adsorption should be accelerated at elevated temperature.

3.2. Adsorption thermodynamics

At equilibrium the adsorption process is considered to be at dynamic state in which the rate of the adsorption process equals that of the desorption process. Adsorption equilibrium is governed by several factors such as the nature of adsorbates and adsorbents as well as the solution composition and temperature.

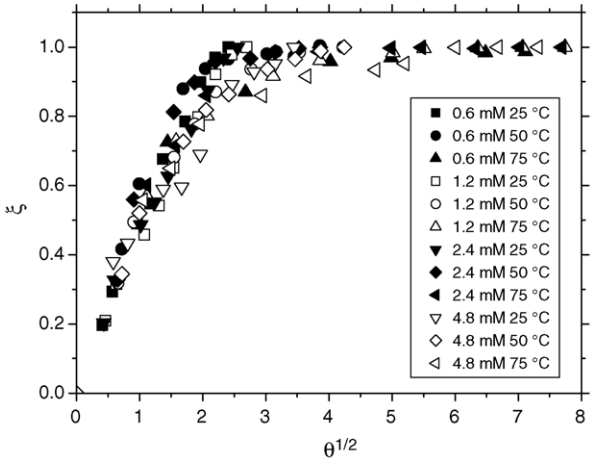

Fig. 4. Plot of ξ vs. $\theta^{1/2}$. Concentration refers to the initial BBF concentration.

3.2.1. Effect of solution pH

The pH of a solution is of significance for its effect on the adsorbent, as well as on the adsobate. Both adsorbent and adsorbate may have functional groups that can be protonated or deprotonated to produce different surface charges in solutions at different pH. This results in the electrostatic attraction or repulsion between charged adsorbates and adsorbents.

The effect of solution pH on the equilibrium adsorption amount is shown in Fig. 5. It is demonstrates that the adsorption decreases with increasing pH because of the electrostatic repulsion between the sulfonate groups of BBF and the negatively charged xerogel surface. Generally, the adsorption decreases with increasing pH for anionic dyes [13,15,19,29], while it increases with increasing pH for cationic dyes [14,30].

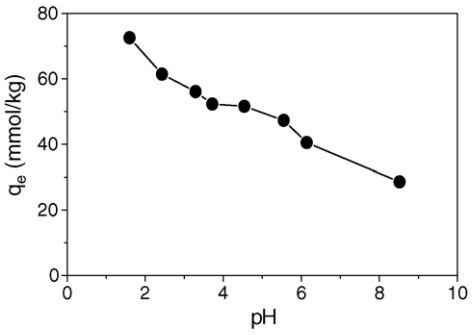

Fig. 5. Effect of pH on the adsorption. Initial BBF concentration is 2.4 mM; initial KNO_3 concentration is 0.25 M; adsorption temperature is 25 °C.

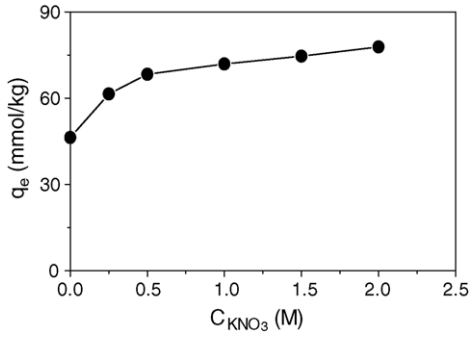

Fig. 6. Effect of ionic strength on the adsorption. Initial BBF concentration is 2.4 mM; initial HCl concentration is 0.01 M; adsorption temperature is 25 °C.

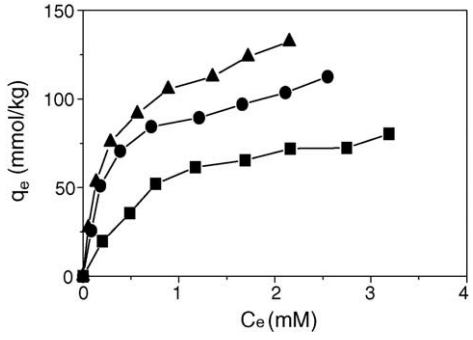

Fig. 7. Adsorption isotherms. Initial HCl concentration is 0.01 M; initial KNO_3 concentration is 0.25 M. (■) 25 °C (●) 50 °C and (▲) 75 °C.

3.2.2. Effect of ionic strength

The effect of ionic strength on the equilibrium adsorption amount is demonstrated in Fig. 6. It is shown that the adsorption increases with the increase in solution ionic strength. For the adsorption of BBF by soils and malachite green by husk-based activated carbon, the adsorption was also found to increase with increasing ionic strength [13,30].

3.2.3. Effect of BBF concentration and temperature—adsorption isotherms

The adsorption isotherms for BBF by the mesoporous xerogel at three different temperatures are shown in Fig. 7. The equilibrium adsorption amount increases with increasing temperature. Similar results were reported for the adsorption of malachite green on rice husk-based active carbon [30], basic red 9 on activated carbon and activated slag [31], three reactive dyes and two acid dyes on modified resin [32].

Langmuir and Freundlich isotherm equations are used to treat the isotherm data. The results are listed in Table 3. Langmuir isotherm gives a better fit than Freundlich isotherm. Similar results were reported for the adsorption isotherms of BBF on soils [13], some acid dyes [19,33], some reactive dyes [15,16,19], and one direct dye [19] on chitosan.

3.2.4. Estimation of the thermodynamics parameters

The Gibbs free energy change of the adsorption process is related to the equilibrium constant by the following equation:

$$\Delta G^\circ = -RT\ln K_c \tag{9}$$

K_c can be calculated according to the following equation [19,34]:

$$K_c = \frac{C_{Ae}}{C_e} \tag{10}$$

where K_c is the equilibrium constant, C_{Ae} the equilibrium amount of BBF (mmol) adsorbed on the adsorbent per liter of the solution, and C_e is the equilibrium concentration (mmol L^{-1}) of BBF in the solution. The initial part of the adsorption isotherm in which q_e versus C_e is linear is used to estimate K_c.

The enthalpy change (ΔH°) and entropy change (ΔS°) for adsorption are assumed to be temperature independent [35,36] and the Gibbs free energy change (ΔG°) is related to the enthalpy and entropy change by the following equation:

$$\Delta G^\circ = \Delta H^\circ - T\Delta S^\circ \tag{11}$$

A study on the temperature dependence of adsorption gives valuable information about the enthalpy and entropy changes during adsorption. The relationship between ΔG° and T is given in Fig. 8. The estimated adsorption thermodynamic parameters are listed in Table 4.

The negative value of ΔG° indicates that the adsorption of BBF on the xerogel is spontaneous for the temperature range evaluated, which is usually the case for many adsorption systems in solution. The positive value of ΔH° shows that the adsorption is endothermic, so raising temperature leads to a higher adsorption of BBF at equilibrium. Positive ΔH° values were also reported for the adsorption of basic red 9 on activated carbon and activated slag [31] and some reactive and acid dyes on modified resin [32]. The positive value of ΔS° indicates a decrease in the order of the system and is similar to the adsorption of basic red 9 on activated

Table 3
Langmuir and Freundlich isotherm constants at different temperature

Temperature (°C)	Langmuir[a]			Freundlich[b]		
	q_m (mmol kg^{-1})	K_L ($mmol^{-1}$)	r	K_F	$1/n$	r
25	96.5 ± 2.7	1.33 ± 0.14	0.996	49.7 ± 2.2	0.484 ± 0.050	0.969
50	120.9 ± 4.3	3.18 ± 0.52	0.996	84.3 ± 5.0	0.381 ± 0.049	0.954
75	144.1 ± 4.8	3.61 ± 0.51	0.998	105.8 ± 5.4	0.397 ± 0.037	0.975

[a] Linear Langmuir equation: $C_e/q_e = 1/(K_L q_m) + C_e/q_m$.
[b] Linear Freundlich equation: $\ln q_e = \ln K_F + (1/n)\ln C_e$.

Table 4
Thermodynamic parameters for the adsorption

Temperature (°C)	K_c	ΔG° (kJ mol^{-1})	ΔH° (kJ mol^{-1})	ΔS° (J mol^{-1} K^{-1})	r
25	1.53 ± 0.12	-1.64 ± 0.19			
50	5.72 ± 0.09	-4.66 ± 0.04	28.5 ± 8.4	100.4 ± 25.9	-0.968
75	8.14 ± 0.55	-5.95 ± 0.20			

carbon and activated slag [31], ethyl(hydroxyethyl)cellulose on trichloromethylsilane treated silica particle [35], 2,2′,3,3′,4,5,6-heptachlorobiphenyl on fly ash [21], some reactive and acid dyes on modified resin [32].

3.2.5. Interaction between BBF and xerogel surface

The competitive adsorption process in aqueous solutions is affected by many factors resulting from adsorbents, adsorbates, and solvent properties. The pore structure of the adsorbent, its energetic heterogeneity, and surface chemical properties (functional groups, surface charge, hydrophilic and hydrophobic nature) are the main factors influencing adsorption equilibria. For a given adsorbent, the adsorption of different adsorbates is a function of solubility, polarity, structure, mass, and size of the molecules. The average pore size of the mesoporous hybrid gel used in our experiments is 2.11 nm, while the dimension of BBF is 1.07 nm × 1.47 nm × 1.88 nm [10]. Thus, BBF ions can easily enter the pores of the mesoporous hybrid gel. The adsorption of BBF on the mesoporous hybrid gel is schematically demonstrated in Fig. 9. There can be three types of interactions responsible for the adsorption: (1) hydrogen bonding; (2) electrostatic attraction; (3) hydrophobic interaction. They belong to noncovalent interactions, which have been reported to play an important role in molecular recognition [37]. Noncovalent interactions are known to act at distances of several angstroms or even tens of angstroms.

As can be seen from Fig. 9, there is a hydrogen bonding between BBF and the gel surface. Our previous work demonstrated that the hydrogen bonding is not a dominant mechanism for the organic dye adsorption on silica or hybrid xerogels [7,8,38].

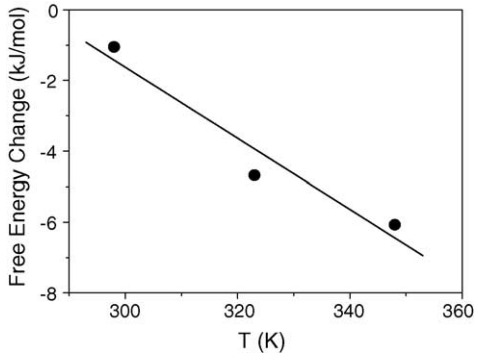

Fig. 8. The standard free energy change of adsorption as a function of temperature. Initial HCl concentration is 0.01 M; initial KNO_3 concentration is 0.25 M.

There exist three kinds of silanol groups (isolated, geminal, and vicinal) [39,40] and propyl groups on the surface of the hybrid gel used in our study. In aqueous solutions, the silanol groups can be protonated or deprotonated depending on the solution pH, which results in the corresponding changes of the surface charge. At low pH, for instance, the protonated gel surface increases the electrostatic attraction between BBF anion and the gel surface, causing the observed increase in BBF adsorption. For the adsorption of reactive red 189 (an anionic dye) on chemical cross-linked chitosan beads, the adsorption capacity increases largely with decreasing pH, and the adsorption mechanism is suggested to be the electrostatic interaction [15]. Effect of pH on the adsorption in Fig. 5 confirms a role of electrostatic interaction.

Electrostatic interaction is known to decrease with the increase in ionic strength probably because of the suppression of the electric double layer [15,41], while hydrophobic attraction increases due to the "salting-out" effect [42]. In our experiments, the equilibrium adsorption amount was found to increase with the increase in solution ionic strength, suggesting the importance of the hydrophobic attraction on the adsorption. Our previous work demonstrated that the adsorption capacity of some organic dyes on hybrid gels is much higher than that on pure silica gels [7,8,38], confirming that the hydrophobic interaction between the surface organic groups of the hybrid gels and the organic dyes plays an important role in adsorption. This is consistent with the

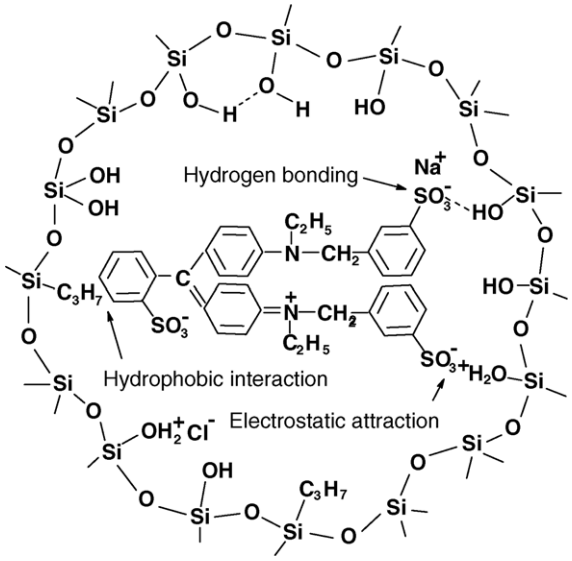

Fig. 9. Schematic diagram of interactions between BBF and xerogel surface.

previous studies where hydrophobicity enhances the adsorption of some organic species by the modified silica [35,43].

4. Summary

The use of a mesoporous hybrid xerogel for the adsorption of an organic dye from aqueous solution has been examined. The results are summarized as follows:

(1) The adsorption kinetics can be well described by the pseudo second-order kinetic model. Initial adsorption rate increases with the increase in initial BBF concentration and temperature. Equilibrium time decreases with the increase in temperature, while the initial dye concentration does not have an obvious effect.
(2) The internal diffusion of BBF into the xerogel is the rate-limiting step of the overall adsorption process.
(3) The equilibrium adsorption amount is found to increase with the increase in initial BBF concentration, temperature, solution acidity, and ionic strength. The adsorption isotherms can be well described with Langmuir equation.
(4) The negative value of the Gibbs free energy change of the adsorption indicates that the adsorption is spontaneous. The positive value of the enthalpy change of the adsorption shows that the adsorption is an endothermic process. Thus, raising the temperature leads to higher BBF adsorption at equilibrium.
(5) Electrostatic attraction and hydrophobic interaction are found to be the dominant interactions between BBF and xerogel surface.

Acknowledgements

This work was financially supported by KOSEF through National Core Research Center for Nanomedical Technology (R15-2004-024-00000-0), and Fujian Provincial Science and Technology Creation Foundation for Young Researchers (2001J023), PR China.

References

[1] P.B. Venuto, Organic catalysis over zeolites: a perspective on reaction paths within micropores, Microporous Mater. 2 (1994) 297–411.
[2] J. Deere, E. Magner, J.G. Wall, B.K. Hodnett, Adsorption and activity of proteins onto mesoporous silica, Catal. Lett. 85 (2003) 19–23.
[3] J. Deere, E. Magner, J.G. Wall, B.K. Hodnett, Adsorption and activity of cytochrome *c* on mesoporous silicates, Chem. Commun. (2001) 465–466.
[4] X. Feng, G.E. Fryxell, L.-Q. Wang, A.Y. Kim, J. Liu, K.M. Kemner, Functionalized monolayers on ordered mesoporous supports, Science 276 (1997) 923–925.
[5] R.I. Nooney, M. Kalyanaraman, G. Kennedy, E.J. Maginn, Heavy metal remediation using functionalized mesoporous silicas with controlled macrostructure, Langmuir 17 (2001) 528–533.
[6] C. Cooper, R. Burch, Mesoporous materials for water treatment processes, Water Res. 33 (1999) 3689–3694.
[7] Z. Wu, H. Joo, I.-S. Ahn, S. Haam, J.-H. Kim, K. Lee, Organic dye adsorption on mesoporous hybrid gels, Chem. Eng. J. 102 (2004) 277–282.
[8] Z. Wu, I.-S. Ahn, J.-H. Kim, K. Lee, Enhancing the organic dye adsorption on porous xerogels, Colloids Surf. A 240 (2004) 157–164.
[9] D.A. Kron, B.T. Holland, R. Wipson, C. Maleke, A. Stein, Anion exchange properties of a mesoporous aluminophosphate, Langmuir 15 (1999) 8300–8308.
[10] H. Tamai, T. Yoshida, M. Sasaki, H. Yasuda, Dye adsorption on mesoporous activated carbon fiber obtained from pitch containing yttrium complex, Carbon 37 (1999) 983–989.
[11] M. Flury, H. Fluher, Brilliant blue FCF as a dye tracer for solute transport studies—a toxicological overview, J. Environ. Qual. 23 (1994) 1108–1112.
[12] H. Ketelsen, S. Meyer-Windel, Adsorption of brilliant blue FCF by soils, Geoderma 90 (1999) 131–145.
[13] J. German-Heins, M. Flury, Sorption of brilliant blue FCF in soils as affected by pH and ionic strength, Geoderma 97 (2000) 87–101.
[14] M. Dogan, M. Alkan, Adsorption kinetics of methyl violet onto perlite, Chemosphere 50 (2003) 517–528.
[15] M.S. Chiou, H.Y. Li, Adsorption behavior of reactive dye in aqueous solution on chemical cross-linked chitosan beads, Chemosphere 50 (2003) 1095–1105.
[16] M.S. Chiou, H.Y. Li, Equilibrium and kinetic modeling of adsorption of reactive dye on cross-linked chitosan beads, J. Hazard. Mater. 93 (2002) 233–248.
[17] Z. Aksu, S. Tezer, Equilibrium and kinetic modelling of biosorption of Remazol Black B by *Rhizopus arrhizus* in a batch system: effect of temperature, Process Biochem. 36 (2000) 431–439.
[18] Z. Aksu, Biosorption of reactive dyes by dried activated sludge: equilibrium and kinetic modeling, Biochem. Eng. J. 7 (2001) 79–84.
[19] M.S. Chiou, P.Y. Ho, H.Y. Li, Adsorption of anionic dyes in acid solutions using chemically cross-linked chitosan beads, Dyes Pigments 60 (2004) 69–84.
[20] C.Y. Chang, W.T. Tsai, C.H. Ing, C.F. Chang, Adsorption of polyethylene glycol (PEG) from aqueous solution onto hydrophobic zeolite, J. Colloid Interface Sci. 260 (2003) 273–279.
[21] H. Nollet, M. Roels, P. Lutgen, P. Van der Meeren, W. Verstraete, Removal of PCBs from wastewater using fly ash, Chemosphere 53 (2003) 655–665.
[22] M. Sarkar, P.K. Acharya, B. Bhattacharya, Modeling the adsorption kinetics of some priority organic pollutants in water from diffusion and activation energy parameters, J. Colloid Interface Sci. 266 (2003) 28–32.
[23] S.-Y. Mak, D.-H. Chen, Fast adsorption of methylene blue on polyacrylic acid-bound iron oxide magnetic nanoparticles, Dyes Pigments 61 (2004) 93–98.
[24] K.G. Bhattacharyya, A. Sharma, *Azadirachta indica* leaf powder as an effective biosorbent for dyes: a case study with aqueous Congo red solutions, J. Environ. Manage. 71 (2004) 217–229.
[25] X. Yang, B. Al-Duri, Kinetic modeling of liquid-phase adsorption of reactive dyes on activated carbon, J. Colloid. Interface Sci. 287 (2005) 25–34.
[26] M. Dogan, M. Alkan, A. Turkyilmaz, Y. Ozdemir, Kinetics and mechanism of removal of methylene blue by adsorption onto perlite, J. Hazardous Mater. 109 (1–3) (2004) 141–148.
[27] Z. Al-qodah, Adsorption of dyes using shale oil ash, Water Res. 34 (17) (2000) 4295–4303.
[28] M. Dogan, M. Alkan, Y. Onganer, Adsorption of methylene blue from aqueous solution onto perlite, Water Air Soil Pollut. 120 (2000) 229–248.
[29] M.A. Al-Ghouti, M.A.M. Khraisheh, S.J. Allen, M.N. Ahmad, The removal of dyes from textile wastewater: a study of the physical characteristics and adsorption mechanisms of diatomaceous earth, J. Environ. Manage. 69 (2003) 229–238.

[30] Y. Guo, S. Yang, W. Fu, J. Qi, R. Li, Z. Wang, H. Xu, Adsorption of malachite green on micro- and mesoporous rice husk-based active carbon, Dyes. Pigments 56 (2003) 219–229.
[31] V.K. Gupta, I. Ali, D.S. Mohan, Equilibrium uptake and sorption dynamics for the removal of a basic dye (basic red) using low-cost adsorbents, J. Colloid Interface Sci. 265 (2003) 257–264.
[32] Y. Yu, Y.Y. Zhuang, Z.H. Wang, M.Q. Qiu, Adsorption of water-soluble dyes onto modified resin, Chemosphere 54 (2004) 425–430.
[33] Y.C. Wong, Y.S. Szeto, W.H. Cheung, G. Mckay, Adsorption of acid dyes on chitosan – equilibrium isotherm analyses, Process Biochem. 39 (2004) 695–704.
[34] P. Kongkachuichay, A. Shitangkoon, N. Chinwongamorn, Thermodynamics of adsorption of laccaic acid on silk, Dyes. Pigments 53 (2002) 179–185.
[35] S. Kapsabelis, C.A. Prestidge, Adsorption of ethyl(hydroxyethyl)cellulose onto silica particles: the role of surface chemistry and temperature, J. Colloid Interface Sci. 228 (2000) 297–305.
[36] P. Jenkins, J. Ralston, The adsorption of a polysaccharide at the talc-aqueous solution interface, Colloids Surf. A 139 (1998) 27–40.
[37] K. Muller-Dethlefs, P. Hobza, Noncovalent interactions: a challenge for experiment and theory, Chem. Rev. 100 (2000) 143–167.
[38] Z. Wu, K. Lee, Preparation of templated organic/inorganic xerogels and their organic dye adsorption behavior in aqueous solutions, 225th American Chemical Society Meeting, New Orleans, USA, 2003, INOR 0809.
[39] C.J. Brinker, G.W. Scherer, Sol–Gel Science: The physics and Chemistry of Sol–Gel Processing, Academic Press, Boston, 1990, pp. 617–628.
[40] J.C. Diniz da Costa, G.Q. Lu, V. Rudolph, Y.S. Lin, Novel molecular sieve silica (MSS) membranes: characterisation and permeation of single-step and two-step sol–gel membranes, J. Membr. Sci. 198 (2002) 9–21.
[41] R.H. Al-Shakhshir, F.E. Regnier, J.L. White, S.L. Hem, Contribution of electrostatic and hydrophobic interactions to the adsorption of proteins by aluminium-containing adjuvants, Vaccine 13 (1995) 41–44.
[42] J. Wang, P. Somasundaran, D.R. Nagaraj, Adsorption mechanism of guar gum at solid–liquid interfaces, Miner. Eng. 18 (2005) 77–81.
[43] R. Makote, M.M. Collinson, Organically modified silicate films for stable pH sensors, Anal. Chim. Acta 394 (1999) 195–200.